Analytical Biochemistry 583 (2019) 113339

Contents lists available at ScienceDirect

Analytical Biochemistry

journal homepage: www.elsevier.com/locate/yabio

# Comparison of composition-gradient sedimentation equilibrium and composition-gradient static light scattering as techniques for quantitative characterization of biomolecular interactions: A case study

Fumio Arisaka[a], Youichi Niimura[b], Allen P. Minton[c,*]

[a] Graduate School of Bioscience and Biotechnology, Tokyo Institute of Technology, Yokohama, 226-8503, Japan
[b] Department of Bio-Science, Tokyo University of Agriculture, Setagaya-ku, Tokyo, 156-8502, Japan
[c] Laboratory of Biochemistry & Genetics, National Institute of Diabetes, Digestive, and Kidney Diseases, National Institutes of Health, United States Department of Health and Human Services, Bethesda, MD, 20892, USA

ARTICLE INFO

*Keywords:*
NADH oxidase
Peroxiredoxin
Heteroassociation equilibria

ABSTRACT

The equilibrium hetero-association of NADH oxidase and peroxiredoxin was characterized by means of independently conducted measurements of composition-gradient sedimentation equilibrium and composition-gradient static light scattering. Results obtained from both experiments were quantitatively accounted for by a model according to which a dimer of NADH oxidase forms a 1:1 equilibrium complex with a decamer of peroxiredoxin under the conditions of these experiments. The best-fit equilibrium constants for heteroassociation of the two proteins obtained from the two measurements were found to be identical to well within the uncertainty of estimate of each of the two methods. The relative virtues of each of the methods are discussed.

## 1. Introduction

Many techniques presented in the literature claim to provide quantitative information about the stoichiometry and equilibrium constants governing reversible macromolecular associations in solution (see for example [1–3]). Yet very few associating systems have been studied by multiple independent methods to ascertain whether the same results are obtained independent of the method employed, an essential means of method validation [3,4].

The technique of composition gradient static light scattering (CG-SLS) was introduced in 2005 and has been used to characterize a number of protein self- and heteroassociation equilibria [2,5,6]. More recently, the technique of composition-gradient sedimentation equilibrium (CG-SE) was developed, but has been described only briefly in a book chapter [7]. The present paper thus has two purposes: (1) to more completely describe the method and practice of CG-SE in order to make it accessible to the bioanalytical community, and (2) to demonstrate that both CG-SE and CG-SLS experiments conducted on similarly prepared solutions of proteins obtained from the same source yield evaluations of binding affinity, stoichiometry, and molar mass that are in very good agreement.

The two proteins studied in the present work are NADH oxidase (NADHox) [8] and peroxiredoxin (Prx) obtained from *Amphibacillus xylanus* [9]. These proteins have been studied intensively by Niimura and coworkers [8–11]. The self- and hetero-interactions of the two proteins have been studied by means of surface plasmon resonance, dynamic light scattering, and sedimentation velocity [11]. However, these methods are not direct measures of self- or hetero-association, as they report solution properties that vary with association in an indirect and incompletely defined fashion. In the following, we report the results and analysis of CG-SE and CG-SLS experiments providing direct measurement of the weight-average molar mass of total protein at equilibrium and its dependence upon solution composition, analysis of which yields molar mass of each of the two interacting proteins as well as the association scheme and equilibrium constant(s).

## 2. Materials

NADHox and Prx were obtained from *Amphibacillus xylanus* and purified as described previously [9,12]. Solutions of each protein were prepared in buffers containing 50 mM HEPES and 300 mM ammonium sulfate at pH 7.0. The density increment $d\rho/dw$, where $\rho$ denotes solution density and $w$ denotes w/v concentration, of each protein was measured via densitometry and found to have an equal value of 0.245 for both. The specific extinction coefficient $A_{280}$ (l/g-cm) was determined to be 1.18 for Prx and 1.90 for NADHox. The refractive

* Corresponding author. Building 8, Room 226, NIH, Bethesda, MD, 20892, USA.
*E-mail address:* allenm@niddk.nih.gov (A.P. Minton).

https://doi.org/10.1016/j.ab.2019.06.010
Received 22 April 2019; Received in revised form 7 June 2019; Accepted 11 June 2019
Available online 15 July 2019
0003-2697/ 

increment $dn/dw$ for both proteins was taken to be equal to a consensus value 0.185 $cm^3/g$ at 660 nm [13].

### 2.1. Analytical methods

*Composition dependence of species in a mixture of self- and hetero-associating proteins.* Consider a solution containing two proteins, A and B, which may exist as an arbitrary number of solute species, denoted by $A_iB_j$, at equilibrium. (Note that homo-oligomers of A or B are special cases of $A_iB_j$ such that one of the two subscripts is equal to 0.) The molar concentration of each species at equilibrium is given by

$$c_{ij} = K_{ij} c_{10}^{i} c_{01}^{j} \tag{1}$$

where $c_{10}$ and $c_{01}$ respectively denote the equilibrium concentrations of monomeric A and B, and $K_{10} = K_{01} = 1$. The total molar concentration of A in the solution is then given by

$$c_{A,tot} = \frac{w_{A,tot}}{M_A} = \sum_{i,j} i c_{ij} \tag{2}$$

and that of B given by

$$c_{B,tot} = \frac{w_{B,tot}}{M_B} = \sum_{i,j} j c_{ij} \tag{3}$$

where $w_{A,tot}$ and $w_{B,tot}$ respectively denote the total w/v concentrations of A and B. Next consider the solution created by mixing volume fraction $f_B$ of a solution of B at w/v concentration $w_B^o$ and volume fraction $(1 - f_B)$ of a solution of A at w/v concentration $w_A^o$. The total concentrations of A and B in this solution mixture will be given by

$$w_{A,tot} = (1 - f_B) w_A^o \tag{4}$$

and

$$w_{B,tot} = f_B w_B^o \tag{5}$$

Thus for any proposed self- and/or hetero-association scheme that is characterized by a specific choice of species and specified values of $w_A^o$, $w_B^o$, $M_A$, $M_B$, and all $K_{ij}$, equations (1)–(3) may be analytically or numerically solved to yield values of $c_{10}$ and $c_{01}$, and then via equation (1), all $c_{ij}$ as functions of $f_B$ [14].

*Composition gradient sedimentation equilibrium.* Each of the individual species present in the solution is assumed to contribute to a total measurable quantity $S$ (for signal), such as absorbance, in proportion to its molar concentration and composition[1].

$$S = \sum_{i,j} s_{ij} c_{ij} \tag{6}$$

where

$$s_{ij} = i s_A M_A + j s_B M_B \tag{7}$$

Here $s_{ij}$ and $c_{ij}$ respectively denote the specific signal and molar concentration of $A_iB_j$, $s_A$ and $s_B$ respectively denote the specific signal (signal per unit concentration) of pure A and B, and $M_A$ and $M_B$ respectively denote the molar mass of monomeric A and B.

When the solution is centrifuged to sedimentation equilibrium at an angular velocity $\omega$ and temperature $T$, the equilibrium gradient of signal $S(r)$ is described by

$$\frac{d \ln S}{dr^2} = \frac{M_S^* \omega^2}{2RT} \tag{8}$$

where $R$ denotes the molar gas constant and $M_S^*$ denotes the signal-average buoyant molar mass, given by

$$M_S^* = \frac{\sum_{i,j} M_{ij}^* s_{ij} c_{ij}}{\sum_{i,j} s_{ij} c_{ij}} \tag{9}$$

$M_{ij}^*$ denotes the buoyant molar mass of species $A_iB_j$, given by

$$M_{ij}^* = i M_A^* + j M_B^* = i M_A \frac{d\rho}{dw_A} + j M_B \frac{d\rho}{dw_B} \tag{10}$$

Thus given the values of $\omega$, $T$, $M_A$, $M_B$, $d\rho/dw_A$, $d\rho/dw_B$, $w_A^o$, $w_B^o$ and all $K_{ij}$, equations (1)–(8) permit the value of $M_S^*$ to be calculated as a function of $f_B$ [7].

*Composition gradient light scattering.* For a thermodynamically ideal solution containing a mixture of species, all of which are small relative to the wavelength of incident light, the angle-independent intensity of scattering of vertically polarized light is given by

$$R/K_{opt} = \sum_{i,j} \left( \frac{dn}{dw_{ij}} \right)^2 M_{ij}^2 c_{ij} \tag{11}$$

where $R/K_{opt}$ denotes the Rayleigh ratio in units of the optical constant $K_{opt}$,

$$M_{ij} = i M_A + j M_B \tag{12}$$

$$\frac{dn}{dw_{ij}} = \frac{i M_A}{M_{ij}} \frac{dn}{dw_A} + \frac{j M_B}{M_{ij}} \frac{dn}{dw_B} \tag{13}$$

and

$$K_{opt} = 4\pi^2 n_0^2 \lambda_0^{-4} N_A^{-1} \tag{14}$$

where $n_0$ denotes the refractive index of solvent, $\lambda_0$ the wavelength of incident light, and $N_A$ Avogadro's number [6]. Thus, given the values of these constants, $dn/dw_A$, $dn/dw_B$, $w_A^o$, $w_B^o$, $M_A$, $M_B$, and all $K_{ij}$, equations (1-5) and (11-14) permit the value of $R/K_{opt}$ to be calculated as a function of $f_B$.

*Modeling of data.* Combined models for equilibrium association and either composition-dependent sedimentation equilibrium or composition-dependent light scattering were fit to data by means of nonlinear least squares using user-written scripts and functions written in MATLAB (Mathworks, Natick MA) that may be obtained upon request from the corresponding author. The uncertainty of the best-fit value of each parameter was determined via parameter scanning [15].

### 2.2. Experimental methods

*Composition gradient sedimentation equilibrium.* Stock solutions of NADHox and Prx were prepared in the buffer specified above, with w/v concentrations equal to 0.25 and 0.40 mg/ml respectively. Then solution mixtures were prepared with the following volume fractions of Prx solution ($f_{Prx}$): 0, 0.2, 0.4, 0.6, 0.8, and 1.0. 70 μl of each solution were loaded into sample compartments of six hole centerpieces and 80 μl of buffer loaded into the corresponding reference compartment. Four sample cells with six hole centerpieces containing all solutions in duplicate were mounted in an eight hole analytical rotor, and were successively centrifuged to sedimentation equilibrium in a Beckman XL-I analytical centrifuge at 20 °C at each of three rotor speeds: 7100, 10500, and 13000 rpm. Samples were periodically scanned at 280 nm at a fixed rotor speed until an equilibrium gradient had been established in all samples, prior to increasing the rotor speed. Raw data files containing tables of $A_{280}$ as a function of radial position $r$, obtained from the final scan at each rotor speed, were subjected to preliminary processing as follows. Data obtained from each sample were plotted in the form of ln $A_{280}$ as a function of $r^2$ and visually inspected to establish that ln $A_{280}$ exhibited a linear or quasilinear dependence upon $r^2$ across the 2 mm column as predicted by equation (8). Then a straight line was fit via linear least-squares to the observed dependence of ln $A_{280}$ upon $r^2$. An example of this procedure is shown in Fig. 1. The slope of the best-fit straight line was taken to be equal to the experimental value of

[1] The investigator should ideally test this assumption for the particular combination of proteins being studied. One method for testing the assumption is described in Ref. [7].

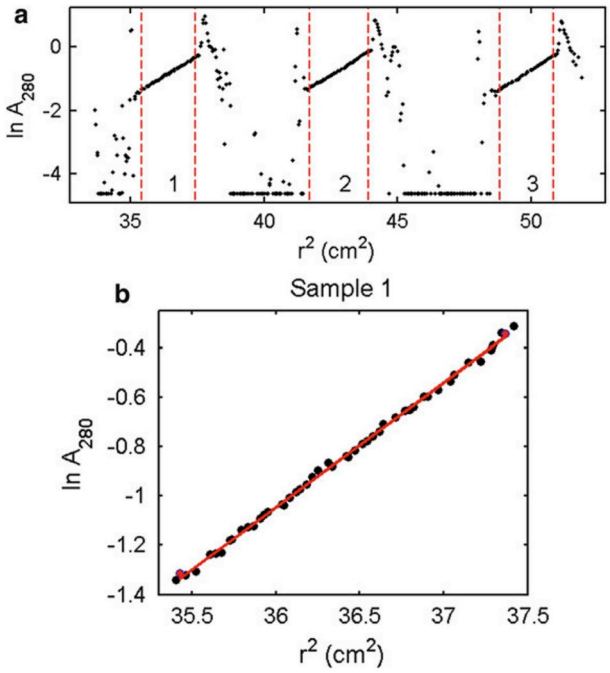


**Fig. 1.** (a). Linearized scan of a sample cell containing a six hole centerpiece (three sample-reference pairs). (b) best fit of a straight line to the linearized data in sample 1. Figure reprinted from Ref. [7] with permission.

$d \ln A_{280}/dr^2$ used in conjunction with equation (8) to calculate the value of the absorbance average buoyant molar mass, $M^*_{abs,av}$, for the particular sample composition ($f_{Prx}$) at that rotor speed. In this fashion, six values of $M^*_{abs,av}$ were obtained for each sample composition (2 replicates at each of 3 rotor speeds).

*Composition gradient static light scattering.* The general technique of measurement is described elsewhere [2], so the following description is limited to particulars of the experiment reported here. Stock solutions of NADHox and Prx were prepared in the buffer specified above, with w/v concentrations equal to 0.53 and 0.99 mg/ml respectively. Solutions and buffer were filtered through a 0.02 μm Whatman Anotop filter, and degassed via centrifugation at 1000 *g* for 15 min immediately prior to light scattering measurement. 9 ml of each solution and buffer were loaded into the three reservoirs of a Calypso II automated three-syringe pump (Wyatt Technology, Santa Barbara CA) connected to a DAWN Heleos II multi-angle light scattering photometer (Wyatt Technology) and T-rEX differential refractometer (Wyatt Technology). Using the Calypso software (Wyatt Technology), the pump was programmed to deliver the time-dependent gradient of concentration of each of the two proteins to the light scattering and concentration detectors shown in Fig. 2. The time period between t = 95 and 370 min may be divided into 11 plateaus of constant concentration, the first plateau containing 0.99 mg/ml of Prx and 0 mg/ml NADHox, and the last plateau containing 0.53 mg/ml Nox and 0 mg/ml NADHox. The intermediate plateaus contain mixtures of the two proteins. Since the concentrations of both proteins are known within each plateau, the corresponding value of $f_{Prx}$ may be calculated. Scattering intensity at 90° was recorded at a rate of 10 $sec^{-1}$, and the mean and standard deviation of the mean of the data in each plateau, corresponding to one value of $f_{prx}$, was automatically calculated and converted to units of $R/K_{opt}$ by the Calypso software.

## 3. Results and analysis

*Model for equilibrium hetero-association.* According to previous work [11], under the conditions of this experiment (in particular, in the presence of 300 mM ammonium sulfate), NADHox is expected to exist as a homodimer with a molar mass of approximately 110 kg, and Prx is expected to exist as a homodecamer with a molar mass of approximately 200 kg. The simplest model for heteroassociation of these two proteins assumes that the association state of each protein separately is constant, and that reversible association between the two proteins under the conditions of these experiments is limited to formation of a single 1:1 complex of NADHox dimer and Prx decamer. Denoting the NADHox dimer by N and the Prx decamer by P, equations (1)–(3) reduce to the following:

$$c_{NP} = K_{11} c_N c_P \tag{15}$$

$$(1 - f_{Prx}) w^o_N = M_N (c_N + c_{NP}) \tag{16}$$

$$f_{Prx} w^o_P = M_P (c_P + c_{NP}) \tag{17}$$

Given values of $w^o_N$, $w^o_P$, $M_A$, $M_B$, and $K_{11}$, equations (15–17) may be solved analytically for the values of $c_N$, $c_P$, and $c_{NP}$ as functions of $f_{Prx}$.

*Composition gradient sedimentation equilibrium.* The results of the experiments described above are summarized in Fig. 3. For the simple 1:1 heteroassociation scheme, and when $d\rho/dw_N = d\rho/dw_P = d\rho/dw$, equations (7), (9) and (10) reduce to

$$a_{NP} = a_N M_N + a_P M_P \tag{18}$$

$$M^*_{abs,av} = \frac{d\rho}{dw} \times \left[ \frac{M_N a_N c_N + M_P a_P c_P + M_{NP} a_{NP} c_{NP}}{a_N c_N + a_P c_P + a_{NP} c_{NP}} \right] \tag{19}$$

where $a_X$ denotes the specific signal (absorbance) of species *X*. Thus given independently determined values of $w^o_N$ (0.25 mg/ml), $w^o_P$ (0.4 mg/ml), $a_N$ (1.90 l/g-cm), $a_P$ (1.18 l/g-cm), $d\rho/dw$ (0.245), and specified values of $M_N$, $M_P$, and $K_{11}$, equations (15–19) permit $M^*_{abs,av}$ to be calculated as a function of $f_{Prx}$. These equations were fit to the data plotted in Fig. 3 via non-linear least-squares to determine the best-fit values and uncertainties of $M_N$, $M_P$, and $\log_{10} K_{11}$ given in Table 1. The dependence of $M^*_{abs,av}$ upon $f_{Prx}$ calculated using these best-fit parameter values is plotted together with the data in Fig. 3.

*Composition gradient static light scattering.* The results of the experiment described above are summarized in Fig. 4. For the simple 1:1 heteroassociation scheme, and when $dn/dw_N = dn/dw_P = dn/dw$, equations (11–13) simplify to

$$R/K_{opt} = \left(\frac{dn}{dw}\right)^2 \times [M_N^2 c_N + M_P^2 c_P + (M_N + M_P)^2 c_{NP}] \tag{20}$$

Thus given independently determined values of $w^o_N$ (0.53 mg/ml), $w^o_P$ (0.99 mg/ml), $dn/dw$(0.185), and specified values of $M_N$, $M_P$, and $K_{11}$, equations (15)–(17) and (20) permit $R/K_{opt}$ to be calculated as a function of $f_{Prx}$. These equations were fit to the data plotted in Fig. 3 via non-linear least-squares to determine the best-fit values and uncertainties of $M_N$, $M_P$, and $\log_{10} K_{11}$ given in Table 1. The dependence of $R/K_{opt}$ upon $f_{Prx}$ calculated using these best-fit parameter values is plotted together with the data in Fig. 4.

## 4. Discussion

The results of modeling presented in Table 1 show that the two methods described here yield essentially identical information of acceptable precision about the molar masses of interacting proteins and the stoichiometry and affinity of reversible heteroassociation, thus mutually validating the methods and experimental procedures employed here. The best-fit values of the molar masses of each of the reactants agree to within experimental uncertainty with the earlier estimates of Arai et al. [11]. These workers earlier concluded on the basis of dynamic light scattering and sedimentation velocity experiments that the NADHox dimer and Prx decamer formed a 1:1 complex in 300 mM ammonium sulfate, but their experiments did not provide information regarding the affinity of complexation.

The composition gradient strategy employed by the two methods compared here is based upon the recognition that information about

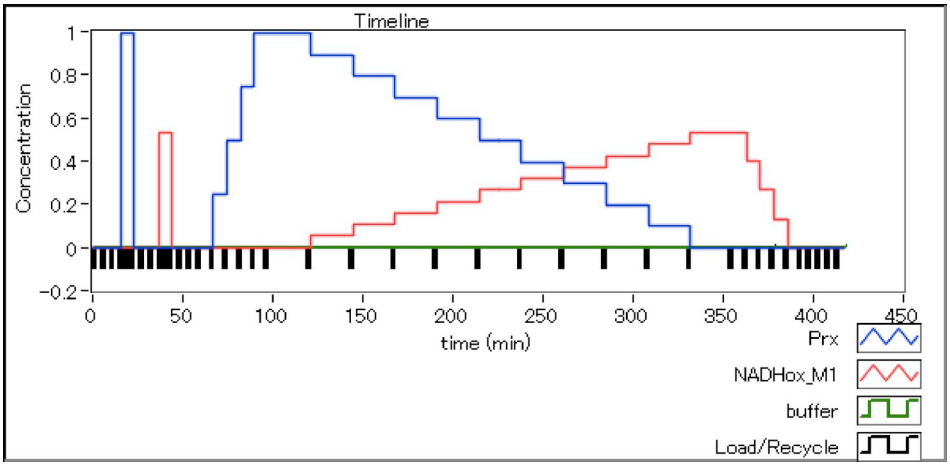


**Fig. 2.** Profile of protein concentration versus time delivered to the light scattering detector. Blue: Prx, Red: NADHox. (For interpretation of the references to colour in this figure legend, the reader is referred to the Web version of this article.)

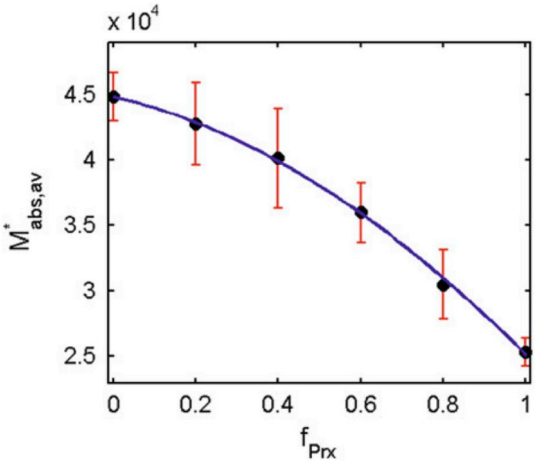


**Fig. 3.** Absorbance-average buoyant molar mass of solution mixtures containing various volume fractions of Prx solution. Symbols: mean of measured values of $M^{*}_{abs,av}$ ± 2 standard deviations of the mean. Blue curve: calculated according to 1-1 association model with best-fit parameter values given in Table 1. Figure reproduced from Ref. [7] with permission. (For interpretation of the references to colour in this figure legend, the reader is referred to the Web version of this article.)

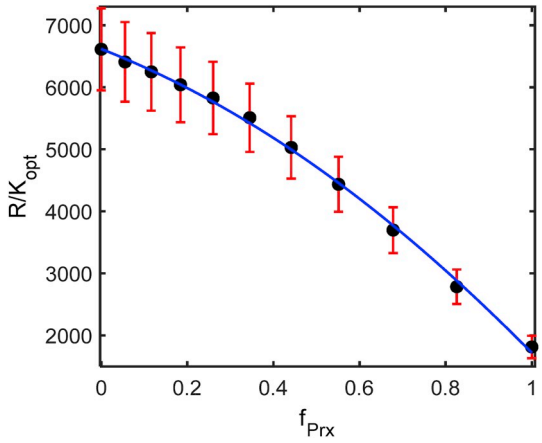


**Fig. 4.** Excess scattering intensity of solution mixtures containing various volume fractions of Prx solution. Symbols: mean of measured values of $R/K_{opt}$ ± 2 standard deviations of the mean. Blue curve: calculated according to 1-1 association model with best-fit parameter values given in Table 1. (For interpretation of the references to colour in this figure legend, the reader is referred to the Web version of this article.)

**Table 1**
Best fit values and uncertainties of undetermined parameters in 1:1 association model to data from composition gradient sedimentation equilibrium experiment shown in Fig. 3, and data from composition gradient light scattering experiment shown in Fig. 4. Indicated uncertainties correspond to 2 standard errors of estimate.

| | CG-SE | CG-SLS |
|---|---|---|
| $M_{Prx}$ (kg) | 103 (+5, −3) | 101 (+15, −10) |
| $M_{NADHox}$ (kg) | 183 (+7, −5) | 204 (+16, −8) |
| $\log_{10} K_{11}$ ($M^{-1}$) | 5.0 (+0.2, −0.4) | 5.0 (+0.2, −0.7) |

hetero-interaction stoichiometry and affinity obtained from a series of mixtures of interacting molecules over the entire range of molar ratios exceeds that obtained by holding the concentration of one reactant constant and varying the concentration of the second reactant [2,5,6], and obviates the need to increase the concentration of the variable reactant beyond the limits of instrumental capabilities or thermodynamic ideality. In Appendix 1 we demonstrate that (1) an assumed heteroassociation stoichiometry of 1:1 provides a superior description of the CG-SE data plotted in Fig. 3 than either the 1:2 or 2:1 stoichiometries, and (2) these data provide a statistically valid measure of the precision to which the value of the equilibrium association constant may be determined.

Each of the two methods described here has perceived advantages and disadvantages. The CG-SE experiment reported here required < 500 µl of each protein solution, whereas the CG-SLS experiment required more than ten times greater volume at comparable concentrations. However, a very recent technological development in light scattering instrumentation (https://www.wyatt.com/products/instruments/udawn-multi-angle-detector-uhplc-sec-mals.html) promises a manifold reduction in the amount of sample required to carry out a CG-SLS study comparable to ours. In contrast, the CG-SE experiment required more than two days of centrifugation to ensure establishment of equilibrium gradients at 3 rotor speeds, whereas the CG-SLS experiment was complete in less than 5 h. However, our CG-SE experiment, the first of its type, was carried out to establish proof of

principle and was not optimized.[2] In Appendix 2 we demonstrate the feasibility of carrying out an optimized experiment of the same type within a span of time comparable to that of a CG-SLS or sedimentation velocity experiment.

The analysis of the composition dependence of the signal average buoyant molar mass as defined in equations [6–8] permits ready application of the technique to the characterization of associations between macromolecules having very different absorbance properties, such as proteins and nucleic acids. In Appendix 3 we demonstrate the sensitivity of the composition dependence of the absorbance-average buoyant molar mass to variation in the specific extinction coefficients of each reactant, and point out how this fact may be exploited to enhance the precision of the GG-SE method.

The equilibrium methods utilized in the present study may be compared with two non-equilibrium methods, sedimentation velocity (SV) and dynamic light scattering (DLS) that have been used to explore equilibrium self- and hetero-associations in solution [11,16–19]. These methods provide direct information about two different measures of transport in solution, namely sedimentation coefficients and diffusion coefficients respectively. While these properties depend upon molar mass, they also depend upon the frictional coefficients of interacting molecules and their complexes, which are functions of the shapes of the solute species. In some cases, the approximation that all solute species – individual protein molecules and their oligomeric complexes - behave as compact quasi-spherical particles is good, and lead to results that are reasonably accurate [17,19]. However, when one is dealing with proteins or complexes whose conformations are ill-defined (for example, intrinsically disordered proteins) or deviate markedly from a compact quasi-spherical conformation, the relationship between molar mass and diffusion or sedimentation coefficients is uncertain. In simple cases, the analysis of composition-dependent hydrodynamic properties can be carried out by allowing the sedimentation and diffusion coefficients of equilibrium species that cannot be independently measured to be treated as floating parameters, the values of which are to be determined by fitting association models to the data [17–19]. However, it should be kept in mind that the more undetermined parameters in any model, the more ambiguous the results of modeling generally become, due to the increased likelihood of correlations between parameter values. In contrast, the equilibrium methods and analyses employed in the present study depend only on the molar mass and independently measurable properties of each of the pure reactants, and therefore do not rely on structural assumptions or additional parameterization.

In summary, the comparative study reported here demonstrates that measurement of the composition dependence of signal-average molar mass by either CG-SE or CG-SLS provides a rigorous, unequivocal, and accurate method for detection and quantitative characterization of reversible macromolecular associations in dilute solution.

## Acknowledgements

The authors thank Mr. Kenichiro Kurono (Shoko Science, Tokyo, Japan) for assistance with the composition gradient light scattering measurements and Dr. D. Mochizuki (Tokyo University of Agriculture) for sample preparation. This work was supported by Japanese Society for the Promotion of Science Grant C 13680736 (FA), Japanese Ministry of Education, Culture, Sports, Science and Technology Grant C 24580125 (YN) and the Intramural Research Program of the National Institute of Diabetes and Digestive and Kidney Diseases (APM).

## Appendix 1. Dependence of experimental result upon reaction scheme and best fit equilibrium constant

The relations set down in the text establish that *in principle*, the composition dependence of the signal-average buoyant molar mass will depend upon the set of association equilibria present in the mixture of reactants. The purpose of the two exercises presented below is to demonstrate that real CG-SE data permit the experimenter to (1) discriminate between alternative association schemes, and (2) determine equilibrium association constants within acceptable precision.

In the text we describe the results of modeling the reported dependence of the signal-average buoyant molar mass upon the volume fraction of Prx solution with a model for a 1:1 association of a dimer of NADHox and a decamer of Prx. In **Panel A of** Fig A1 we replot the experimental data and the best-fit of the 1:1 model. In addition, we plot the best-fits of 1:2 and 2:1 models for heteroassociation of the same two reactant species. The best-fit values of association equilibrium constants and the best-fit sum of squared residuals (SSR) are given in the figure caption. On the basis of visual inspection alone, it may seem that the difference between the three calculated best-fit dependence of $M^{*}_{abs,av}$ upon $f_{Prx}$ is small, but the fractional difference between the best-fit values of SSR is large. Moreover, it may be seen clearly in **Panel B** of the figure that the distributions of residuals obtained from both the 1:2 and 2:1 association models are markedly non-random, indicating systematic rather than random error in the model fit.

As described under methods in the text, the precision of a best-fit parameter value is estimated using the parameter scanning method of Saroff [15]. According to this method, a selected parameter is constrained to each of a series of values deviating from the best-fit value, and for each of these values, a least-squares fit to the data is obtained by variation of the remaining undetermined parameters. If the selected parameter is well-determined by the data, the SSR of each of the constrained fits will exceed that of the unconstrained best-fit by an amount that will generally increase monotonically with the deviation of the constrained value from its best-fit value. The relative probability that the constrained best-fit is statistically indistinguishable from the unconstrained best fit may be estimated using the Fisher F-test for comparison of variances with specified mathematical degrees of freedom. The result of parameter scanning on $\log K_{11}$ is plotted in Fig. A2. The values of $\log K_{11}$ corresponding to 0.5 and 0.05 probability of statistical indistinguishability are traditionally referred to as 50% and 95% confidence limits or 1 and 2 standard errors of estimate respectively. The uncertainty of $\log K_{11}$ obtained from our CG-SE and CG-SLS experiments in text Table 1 correspond to 2 standard errors of estimate.

## Appendix 2. Optimizing a composition gradient – sedimentation equilibrium experiment

The particular experiment described in detail in the text was the very first experiment of its type performed. The purpose of this appendix is to demonstrate that a comparable amount of information regarding hetero-associations may be obtained from experiments using much smaller sample sizes with concomitant reduction in the amounts of reactants needed and the duration of the experiment. Extensive simulations carried out by Chatelier [20] led to the following parameterized estimate of the amount of time required to centrifuge a column of length $\Delta r$ containing a solute of molar mass M from an initially uniform concentration to an equilibrium gradient:

$$t_{eq} = 247(\Delta r)^2 M^{1/3} \quad [A1]$$

[2] For example, a naive protocol for unattended data acquisition at periodic intervals was set up prior to the start of centrifugation, and no attempt was made to establish the shortest time at which sedimentation equilibrium had been established at each rotor speed.

where the equilibration time $t_{eq}$ is given in minutes and $\Delta r$ in cm. According to this estimate, by shortening the column by one-half, equilibration may be accelerated by a factor of 4, in agreement with earlier results of van Holde and Baldwin [21].

Test experiments were carried out as described in the text using reduced volumes (~50 μl/sample) of mixtures of varying proportions of the same solutions of Prx and NADHox. Linearized gradients obtained from some of these samples at different rotor speeds are plotted in Figure A3. The quality of the data shown here is typical of our test samples. The lengths of the sample columns shown in this figure vary from 0.12 to 0.13 cm, compared to the 0.16 cm columns prepared in our initial experiment. A straight line was fit by linear least squares to all the data shown in each panel, and the value of the best-fit slope obtained in each panel, which is proportional to the signal-average buoyant molar mass (text equation [8]) is given in Table A1. The best-fit straight line is plotted as a red line in Figure A3 together with the data. We did not repeat the experiment with shorter columns, but we can simulate the results obtained from shorter columns by fitting a straight line to the bottom half of each column, corresponding to approximately half of the solution volume, or a column length of .06 - .07 cm. The value of the best-fit slope obtained by fitting to the bottom half-column of each data set is also given in Table A1, and the best-fit straight line so obtained is plotted as a dashed blue line in Figure A3. The difference between the slopes obtained by fitting to the full column and half column of a single sample is seen to be less than 2% in all cases, which is considerably less than the uncertainty of estimate of the signal-average buoyant molar mass obtained from modeling replicate samples at multiple rotor speeds (see 2 SD error bars in Text Fig. 3). According to equation [A1], in the worst case – centrifugation from uniform concentration and the highest value of $M$ corresponding to pure NADHox decamer – the .13 cm column should equilibrate in less than 4 h and the (simulated) .065 cm column should equilibrate in about 1 h. These equilibration times will be shorter when one is transitioning from equilibrium at a lower rotor speed to that at a higher rotor speed, and when the weight-average molar mass is less than that of pure NADHox decamer.

We may therefore state with some confidence that a properly optimized CG-SE experiment may yield reliable information about the composition dependence of the buoyant signal-average molar mass within a period of time comparable to the time required to carry out a sedimentation velocity experiment or a CG-SLS experiment.

## Appendix 3. Sensitivity of the composition dependence of signal-average buoyant molar mass to differences in the specific signals of reactants

In Figure A4 we plot the dependence of $M^*_{s,av}$ upon $f_{Prx}$ calculated using text equations [15–19] with the parameter values given in column 1 of text Table 1, plus the following constants: $w^0_N = 0.25$ mg/ml, $w^0_P = 0.4$ mg/ml, and $d\rho/dw = 0.245$ , and three different combinations of $a_N$ and $a_P$, the specific absorbances of pure N and pure P respectively, as indicated in the caption to Figure A4. The three combinations correspond to the experimentally measured ratio of $a_N$ to $a_P$, one quarter of the ratio, and four times the ratio. The results of these calculations indicate that in order to properly interpret the composition dependence of the signal average buoyant molar mass it is essential to obtain accurate values of $a_N$ and $a_P$ under the conditions of the experiment. In the case of an absorbance average, this may be performed readily in the analytical ultracentrifuge by absorbance scanning of the samples containing pure A and pure B at their loading concentrations at the lowest possible rotor speed, prior to the onset of sedimentation, that is, at a uniform concentration. The results further demonstrate that the CG-SE method may be enhanced by absorbance scanning of the samples at multiple wavelengths selected to optimize variations in the values of $a_N$ and $a_P$ and their ratio. Global modeling of the resulting data with a single reaction scheme and multiple predetermined values of $a_N$ and $a_P$ will increase the precision and accuracy of the results of modeling.

## Declaration of competing interests

All authors declare that they have no competing interests.

Table A1
Slopes of best fit straight lines fitting full column and bottom half column data

| | Best-fit slope | | |
|---|---|---|---|
| Panel | Full column fit | Bottom half column fit | % difference |
| A | .589 | .596 | +1.2 |
| B | .878 | .894 | +1.8 |
| C | .515 | .507 | −1.6 |
| D | 1.104 | 1.092 | −1.1 |
| E | 1.680 | 1.649 | −1.8 |

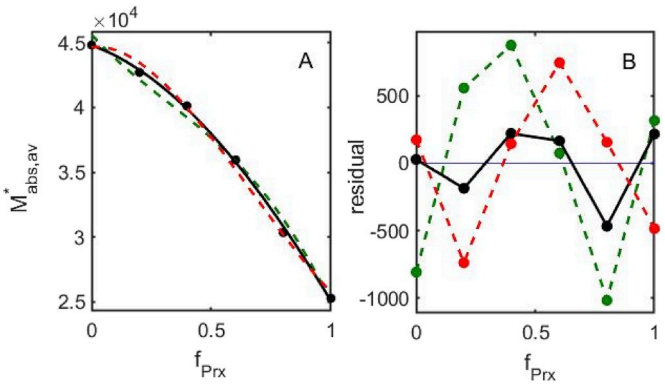


**Fig. A1.** Comparison of three models for heteroassociation of NADHox and Prx. Panel A: Symbols, experimental results as shown in Fig. 1. Curves calculated as described in methods with the following independently measured quantities: $w_N^o$(0.25 mg/ml), $w_P^o$ (0.4 mg/ml), $a_N$ (1.90 l/g-cm), $a_P$ (1.18 l/g-cm), $d\rho/dw$, (0.245), and the best-fit parameters of three different models for the stoichiometry of heteroassociation. Black: 1:1 stoichiometry, $M_P$ = 103 kg, $M_N$ = 183 kg, log $K_{11}$ = 5.0, best fit SSR = 380,404. Red: 1:2 stoichiometry, $M_P$ = 105 kg, $M_N$ = 182 kg, log $K_{12}$ = 10.4, best fit SSR = 1,413,665. Green: 2:1 stoichiometry, $M_P$ = 102 kg, $M_N$ = 186 kg, log $K_{12}$ = 10.1, best fit SSR = 2,873,594. Panel B: symbols are (measured – calculated) values of $M^*_{abs,av}$ for each of the experimental mixtures and the three models described above.

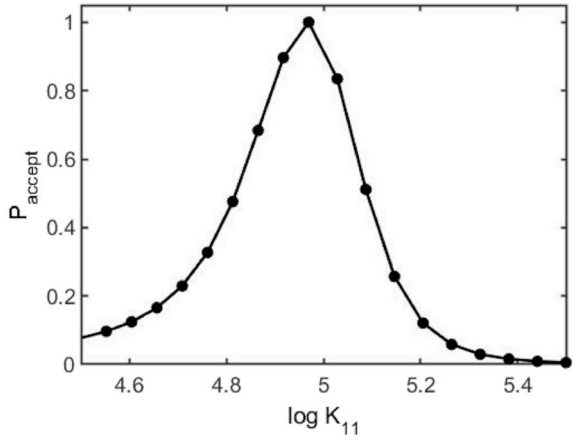


**Fig. A2.** Example of parameter scanning. The probability of relative acceptability (or statistical indistinguishability) of the sum of squared residuals of the best fit of the 1:1 stoichiometry model with the value of log $K_{11}$ constrained to the values indicated on the x-axis.

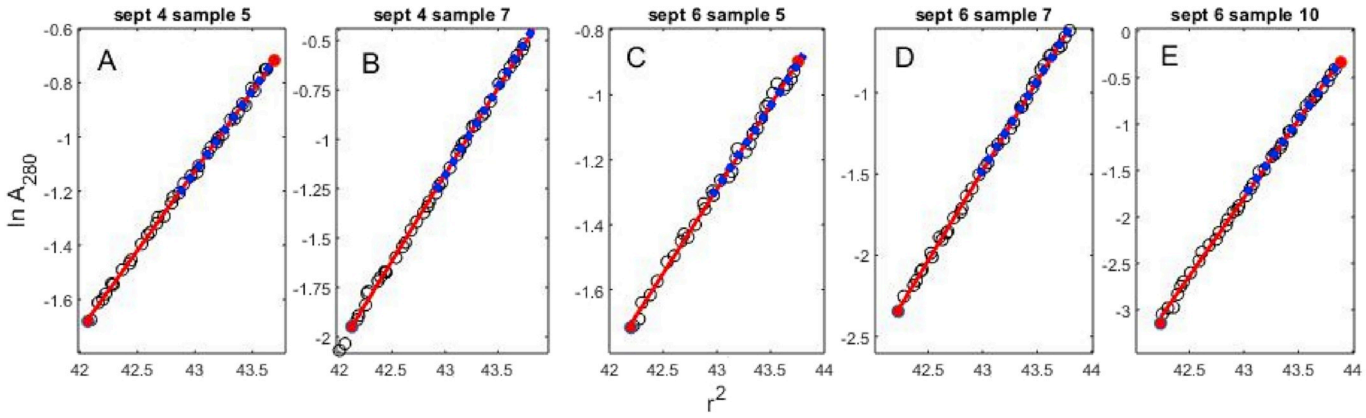


**Fig. A3.** Linearized absorbance scans obtained from test samples. Symbols: experimental data. Red line: best fit straight line to data from full column. Blue dashed line: best fit straight line to data from bottom half-column.

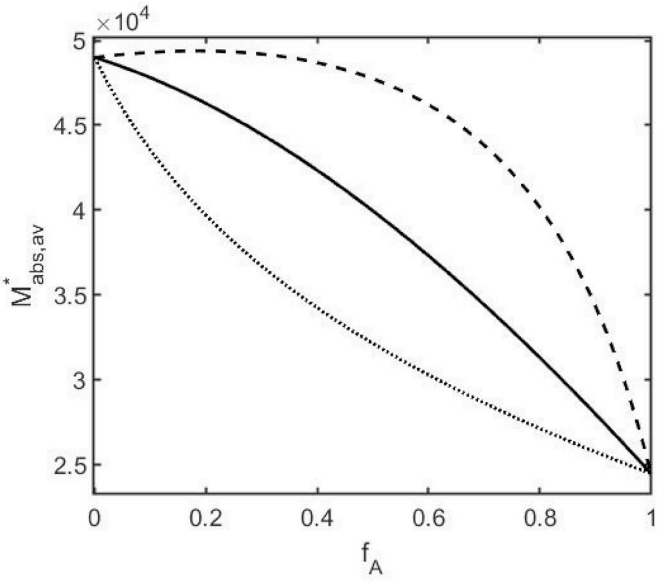


**Fig. A4.** Sensitivity of the composition dependence of $M^*_{abs,av}$ to variation in the specific absorbance of pure reactants. Solid curve: calculated using the experimentally measured values of $a_N$ = 1.18 mg/ml-cm and $a_P$ = 1.9 mg/ml-cm. Dashed curve: $a_N$ = 0.59 mg/ml-cm and $a_P$ = 3.8 mg/ml-cm. Dotted curve: $a_N$ = 2.36 mg/ml-cm and $a_P$ = 0.95 mg/ml-cm.

## References


[1] G.J. Howlett, A.P. Minton, G. Rivas, Analytical ultracentrifugation for the study of protein association and assembly, Curr. Opin. Chem. Biol. 10 (2006) 430–436.

[2] D. Some, Light-scattering-based analysis of biomolecular interactions, Biophys. Revs. 5 (2013) 147–158.

[3] A.P. Yamniuk, J.A. Newitt, M.L. Doyle, F. Arisaka, A.M. Gianetti, P. Hensley, D.G. Myszka, F.P. Schwartz, J.A. Thomson, E. Eisenstein, Development of a model protein interaction pair as a benchmarking tool for the quantitative analysis of 2-site protein-protein interactions, J. Biomol. Tech. 26 (2005) 125–141.

[4] M. Jiménez, G. Rivas, A.P. Minton, Quantitative characterization of weak self-association in concentrated solutions of immunoglobulin G via measurement of sedimentation equilibrium and osmotic pressure, Biochemistry 45 (2007) 13356–13360.

[5] K. Kameyama, A.P. Minton, Rapid quantitative characterization of protein interactions by composition gradient static light scattering, Biophys. J. 90 (2006) 2164–2169.

[6] A.K. Attri, A.P. Minton, Composition gradient static light scattering: a new technique for rapid detection and quantitative characterization of reversible macromolecular hetero-associations in solution, Anal. Biochem. 346 (2005) 132–138.

[7] A.P. Minton, Detection and quantitative characterization of macromolecular heteroassociations via composition gradient sedimentation equilibrium, in: S. Uchiyama, F. Arisaka, W.F. Stafford, T. Laue (Eds.), Analytical Centrifugation. Instrumentation, Software, and Applications, Springer Japan KK, Japan, 2016, pp. 523–532.

[8] Y. Niimura, L.B. Poole, V. Massey, *Amphibacillus xylanus* NADH oxidase and *Salmonella typhimurium* alkyl-hydroperoxide reductase flavoprotein components show extremely high scavenging activity for both alkyl hydroperoxide and hydrogen peroxide in the presence of *S. typhimurium* alkyl hydroperoxide reductase 22-kDa protein component, J. Biol. Chem. 270 (1995) 25645–25650.

[9] Y. Niimura, Y. Nishiyama, D. Saito, H. Tsuji, M. Hidaka, T. Miyaji, T. Watanabe, V. Massey, A hydrogen peroxide-forming NADH oxidase that functions as an alkyl hydroperoxide reductase in *Amphibacillus xylanus*, J. Bacteriol. 182 (2000) 5046–5051.

[10] K. Kitano, Y. Niimura, Y. Nishiyama, K. Miki, Stimulation of peroxidase activity by decamerization related to ionic strength: AhpC protein from *Amphibacillus xylanus*, J. Biochem. 126 (1999) 313–319.

[11] T. Arai, S. Kimata, D. Mochizuki, K. Hara, T. Zako, M. Odaka, M. Yohda, F. Arisaka, S. Kanamaru, T. Matsumoto, S. Yajima, J. Sato, S. Kawasaki, Y. Niimura, NADH oxidase and alkyl hydroperoxide reductase subunit C (peroxiredoxin) from *Amphibacillus xylanus* form an oligomeric assembly, FEBS Open Bio 5 (2015) 124–131.

[12] K. Ohnishi, Y. Niimura, M. Hidaka, H. Masaki, H. Suzuki, T. Uozumi, T. Nishino, Role of cysteine 337 and cysteine 340 in flovoprotein that functions as NADH oxidase from *Amphibacillus xylanus* studied by site-directed mutagenesis, J. Biol. Chem. 270 (1995) 5812–5817.

[13] Wyatt Technology Corp, https://www.wyatt.com/files/tech-notes/instruments/optilab/tn4002a-protein-refractive-index-increment.pdf, (2017).

[14] A.P. Minton, Alternative strategies for the characterization of associations in multicomponent solutions via measurement of sedimentation equilibrium, Prog. Colloid Polym. Sci. 107 (1997) 11–19.

[15] H.A. Saroff, Evaluation of uncertainties for parameters in binding studies: the sum-of-squares profile and Monte Carlo estimation, Anal. Biochem. 176 (1989) 161–169.

[16] J.J. Correia, Analysis of weight-average sedimentation velocity data, Methods Enzymol. 321 (2000) 81–100.
[17] A.D. Hanlon, M.I. Larkin, R.M. Reddick, Free-solution, label-free protein-protein interactions characterized by dynamic light scattering, Biophys. J. 98 (2010) 297–304.
[18] P. Schuck, On the analysis of protein self-association by sedimentation velocity analytical centrifugation, Anal. Biochem. 320 (2003) 104–124.
[19] D. Wu, A.P. Minton, Quantitative characterization of the compensating effects of trimethylamine-N-oxide and guanidine hydrochloride on the dissociation of human cyanmethemoglobin, J. Phys. Chem. B 117 (2013) 9395–9399.
[20] R.C. Chatelier, A parameterized overspeeding method for the rapid attainment of low-speed sedimentation equilibrium, Anal. Biochem. 175 (1988) 114–119.
[21] K.E. Van Holde, R.L. Baldwin, Rapid attainment of sedimentation equilibrium, J. Phys. Chem. 62 (1958) 734–743.